2022 14th International Conference on Measuring Technology and Mechatronics Automation (ICMTMA) | 978-1-6654-9978-1/22/$31.00 ©2022 IEEE | DOI: 10.1109/ICMTMA54903.2022.00162

Performance simulation of lead-free perovskite solar cells

Heng Zhang*, Wenwen Zhang, Yanguo Lu

Xi'an University of Posts and Telecommunications, Xi'an, 710000, China
*corresponding author
E-mail: zhanghishero@163.com

***Abstract*—The solar cell simulation software SCAPS was used to simulate a Sn-based perovskite solar cell with a design structure of Glass substrate/FTO/ZnO/ $CH_3NH_3SnI_3$/Cu_2O/Au. The effects of absorber layer thickness and defect density, as well as the acceptor concentration on the solar cell performance were investigated. From the simulation results, it is known that reducing the defect density of the absorber layer and improving the stability of Sn^{2+} are key issues for future research. When the thickness of $CH_3NH_3SnI_3$ is 500 nm and the defect state is $1\times10^{14}cm^{-3}$, the cell performance is further improved and the optimised cell output characteristics are Voc = 0.917V, Jsc = 33.148 mA·cm^{-2}, FF = 80.02% and PCE = 23.93%.**

Keywords- lead-free; perovskite solar cell; SCAPS simulator; thickness; defect density

I. INTRODUCTION

After decades of development, solar cells have gone through three generations. As the third generation of new solar cells, Perovskite solar cell (PSC) is generally 10^4 ~10^5cm^{-1} due to its high absorption coefficient of absorption layer [1], Exciton has been widely studied for its low binding energy [2], high mobility of carriers [3], and long diffusion length of carriers [4]. The crystal structure of perovskite materials has the general formula ABX3, where A, B and X are different atoms or chemical groups. Usually A is an organic cation, B is a metal ion and X is a halogen group. In the crystal structure of perovskite materials, B ions are coordinated with X ions to form [BX6] octahedra, with B ions at the center of the octahedra and X ions at the six vertices of the octahedra, and A ions filling the centers of the pores between the octahedra. Since it was first reported in 2009, the conversion efficiency of perovskite solar cells has risen from an initial 2.2% to 25.5% [5]. Methylamine-lead halide (MAPbX3, X = Cl, Br, I) is generally considered to be a better performing perovskite material and has been extensively studied in the field of perovskite solar energy due to its high absorption coefficient, bipolar transport properties as well as its long diffusion length and high carrier mobility, however, the toxicity of lead element Pb limits the commercial application of perovskite solar cells with methylamine-lead halide as the absorber layer. Therefore, lead-free perovskite solar cells have become a hot topic of research in the field of photovoltaic technology.

For efficient PSCs, the electron transport layer (ETL) and the hole transport layer (HTL) are important components of the device structure [6]. The electron transport layer is used to form electron-selective contacts with the perovskite absorber layer to increase the photogenerated electron extraction rate and effectively block hole migration towards the cathode. The hole transport layer is used to block electron transport, enhance hole transport and prevent quenching caused by contact between the perovskite active layer and the electrode. The titanium dioxide TiO_2 and sprio-OMeTAD is the most widely used electron- transporting and hole-transporting material in perovskite solar cells. As the preparation of TiO_2 often requires high temperature calcination at 500°C, the high temperature process severely limits the application of TiO_2 in flexible plastic-based cells, while sprio-OMeTAD is more difficult to purify and therefore expensive, increasing the preparation cost. In addition, the unstable properties of TiO_2 and sprio-OMeTAD limit the device performance [7-8].

Based on this, in order to reduce the cost and improve the device performance, this paper designs a Glass substrate/FTO/ZnO/$CH_3NH_3SnI_3$/Cu_2O/Au cell device by using non-toxic $CH_3NH_3SnI_3$ as the perovskite absorber layer and the solar cell simulation software SCAPS as the platform. Power conversion efficiency (PCE), fill factor (FF), short circuit current density (Jsc) and open circuit voltage (Voc) as indicators to discuss the effect of absorber layer thickness and defect density on cell performance. The effects of absorber layer thickness and defect density on cell performance are discussed and used as a basis to design high-efficiency and low-cost Sn-based perovskite solar cells.

II. EXPERIMENT

This paper is based on the solar cell capacitance simulator (SCAPS) [9], a one-dimensional simulation software for different types of solar cells. It is widely used to simulate the device parameters of PSCs and other solar cell structures. The Poisson equation (Eq. (1)), The electron continuum equation (Eq. (2)), and the hole continuum equation (Eq. (3)) are used to obtain the carrier quasi-Fermi energy level, the cell J-V characteristics and the spectral response.

$$\frac{\mathrm{d}}{dx}[\varepsilon(x)\frac{d\psi}{dx}]=q[p(x)-n(x)+N_D^{+}(x)-N_A^{-}(x)+P_t(x)-n_t(x)] \tag{1}$$

$$-\frac{1}{\mathrm{q}}\frac{\mathrm{dJ}_n}{dx}+R_n(x)-G(x)=0 \tag{2}$$

$$\frac{1}{\mathrm{q}}\frac{\mathrm{dJ}_P}{dx}+R_P(x)-G(x)=0 \tag{3}$$

Where ε is the relative permittivity, N_A^+ and N_D^+ are the ionised acceptor concentration and donor concentration, ψ is the electrostatic potential, P_t and n_t denote captured holes and captured electrons respectively, p and n represent free

978-1-6654-9978-1/22/$31.00 ©2022 IEEE
DOI 10.1109/ICMTMA54903.2022.00162

Authorized licensed use limited to: UNIVERSIDADE FEDERAL DO ESPIRITO SANTO. Downloaded on June 14,2022 at 09:47:05 UTC from IEEE Xplore. Restrictions apply.

holes and free electrons respectively, x is the position coordinate, Jn and Jp represent the current densities of electrons and holes respectively, $R_n(x)$ and $R_P(x)$ denote the complex rates of electrons and holes respectively, G(x) is the production rate and q is the electric charge.

The structure of lead-free perovskite solar cell studied in this paper is shown in Figure 1 (a). From top to bottom, it is back electrode Au/hole transport layer Cu_2O/light absorption layer $CH_3NH_3SnI_3$/electron transport layer ZnO/transparent conductive glass FTO. Compared with Ti_2O, ZnO as an electron transport layer is easy to prepare large-area films without high-temperature sintering, and has higher electron mobility [10]. Cu_2O as a hole transport layer has the advantages of non-toxicity, low cost and easy fabrication compared with sprio-OMeTAD. Figure 1 (b) shows the energy level structure and carrier migration diagram. It can be seen from the figure that from the energy level structure, the conduction band position (CB) of the light absorbing layer $CH_3NH_3SnI_3$ is above the ZnO conduction band level, and the valence band position (VB) is above the Cu_2O valence band level. When the light excites the absorption layer, the photogenerated current carriers can be effectively transferred to the conduction band of ETM and the valence band of HTM respectively. It can be seen that ZnO, $CH_3NH_3SnI_3$ and Cu_2O can achieve good energy level matching, which meets the basic requirements of solar cell structure design.

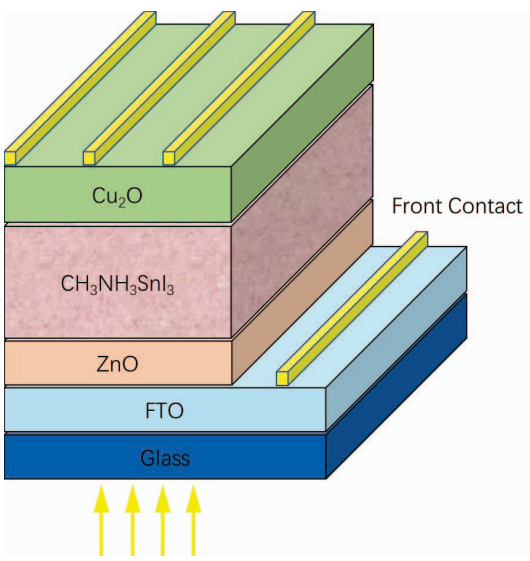

Figure 1. (a) Structure diagram of lead-free perovskite

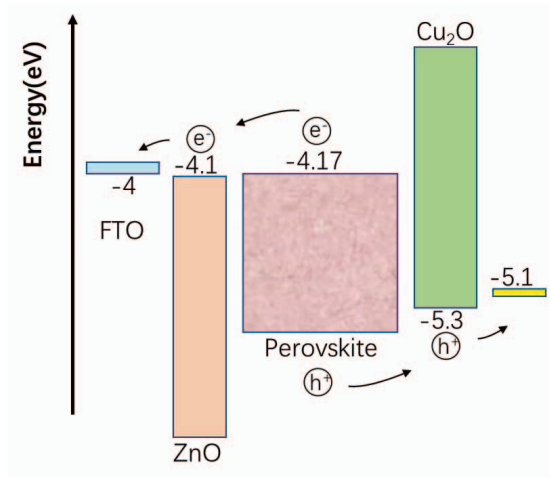

Figure 1. (b) energy level and charge migration diagram

The simulation parameters are set according to reported theoretical and experimental results [11-12], and the specific parameters for each layer configuration are shown in Table 1. where the thickness is denoted by t, the energy band is denoted by Eg, and the electron affinity is denoted by χ. The relative permittivity is εr, and the effective density of states in the conduction and valence bands are Nc and Nv, respectively. μn and μp are the electron mobility and hole mobility, respectively. The applicator concentration, acceptor concentration and trap density are denoted as N_D, N_A and N_t, respectively.

In addition to the parameters shown in the table, the electron/hole thermal velocity of each layer is 10^7 cm/s, the simulated light conditions are AM1.5G, the light intensity is 100 mW/cm^2, and the simulation temperature is set to 300 K. The absorption layer is set to be neutral, Gaussian distributed, with a characteristic energy of 0.1 eV, while the other layers are set to be neutral, single distributed, with electron and hole capture cross sections set at 1×10^{-15}cm^2 for both electrons and holes. In order to reduce the error between the simulation results and the actual results, an interface layer was inserted between the electron transport layer/absorption layer and the absorption layer/hole transport layer, and the two interface defect layers were set to neutral, single type distribution with the energy level positioned 0.6 eV above the top Ev of the valence band, and the total density of defect states was set to 1.0×10^{15}cm^{-3} [13]. This is shown in Table 2. The absorption coefficient (α) is calculated by the equation $\alpha = A\ \alpha(h\text{-}Eg)^{1/2}$ where the perfector Aα is set to a fixed value of 10^5 [14].

Authorized licensed use limited to: UNIVERSIDADE FEDERAL DO ESPIRITO SANTO. Downloaded on June 14,2022 at 09:47:05 UTC from IEEE Xplore. Restrictions apply.

Table 1 Parameters for each layer of the battery device

Parameter	FTO	ZnO	$CH_3NH_3SnI_3$	Cu_2O
t (nm)	100	100	300	420
Eg (eV)	3.5	3.3	1.3	2.17
χ (eV)	4.00	4.10	4.17	3.20
ε_r	9.0	9.0	8.2	7.1
Nc (cm^{-3})	2.2×10^{18}	4×10^{18}	1.0×10^{18}	2.0×10^{17}
Nv (cm^{-3})	1.8×10^{19}	1.0×10^{19}	1.0×10^{18}	1.1×10^{19}
μ_n ($cm^2V^{-1}s^{-1}$)	20.0	100.0	2000.0	200.0
μ_p ($cm^2V^{-1}s^{-1}$)	10.0	25.0	300.0	80
N_D (cm^{-3})	1.0×10^{18}	1.0×10^{18}	0	0
N_A (cm^{-3})	0	0	1.0×10^{14}	1.0×10^{18}
N_t (cm^{-3})	1.0×10^{14}	1.0×10^{15}	3.02×10^{16}	1.0×10^{14}

Table 2 Defect density parameters in the absorber and at the interfaces.

	ETL/Absorber	Absorber/HTM	CH3NH3SnI3
Defect type	Neutral	Neutral	Neutral
σn (cm^{-2})	1.0×10^{-15}	1.0×10^{-15}	2.5×10^{-13}
σp (cm^{-2})	1.0×10^{-15}	1.0×10^{-15}	8.5×10^{-15}
distribution	Single	Single	Gaussian
Et—EV	0.6	0.6	0.65
energy (eV)	-	-	0.1
density (cm^{-3})	1.0×10^{-15}	1.0×10^{-15}	3.02×10^{16}

Based on the initial parameters designed above, the performance parameters of the tin-based perovskite solar cell in the initial state were obtained as follows: Voc = 0.65 V, Jsc = 28.22 mA/cm^2, FF = 73.36% and PCE = 14.9%.

III. Results and Discussion

A. Effect of absorber layer thickness on cell performance

$CH_3NH_3SnI_3$, as the absorber layer of a perovskite solar cell, is a key part in determining the photovoltaic conversion efficiency of the cell. The carrier generation and compounding are mainly directly related to the defect concentration inside the cell and the light energy absorption efficiency of the absorber layer. Because the absorption efficiency of the absorber layer is mainly related to the thickness of the cell, the effect on the cell performance is discussed in this simulation by varying the thickness of the absorber layer. In this paper, the absorber layer thickness is set to vary in the range of 200 to 1000 nm, as shown in Figure2, and the change of thickness on the cell performance.

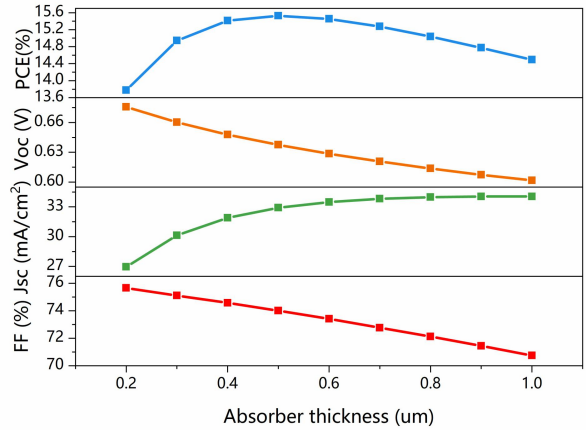

Figure 2. Variation of photovoltaic performance with absorber layer thickness

As observed in Figure 2, Jsc increases sharply up to 700 nm and then the increase becomes slow, with a maximum Jsc of 34 mA/cm^2 obtained at 900 nm, mainly attributed to the large absorption coefficient of the perovskite material [15]. Voc continues to decrease, probably because the thicker absorber layer enhances the carrier recombination [16]. FF also shows a decreasing trend with absorber layer thickness, probably due to the fact that increasing thickness increases the series resistance of the cell [17]. In addition, the PCE increases and then decreases, reaching a maximum at 500 nm, firstly because the thickness of the absorber layer is smaller than the diffusion length of the carriers and therefore most of the ions reach the electrode, however, as the thickness increases, the compounding rate of the carriers increases and therefore the PCE decreases with further increase in thickness [18]. From the simulation results it is clear that the absorber layer thickness is best set at 500 nm.

B.Effect of absorber layer defect density on cell performance

The quality of the $CH_3NH_3SnI_3$ film directly affects the number of photogenerated carriers and therefore the performance of the cell. A larger defect density of states indicates a poorer film quality and the carrier complexation rate will be greater than that produced. This simulation sets the defect of the absorber layer to vary in the range of 1×10^{10}~1×10^{19}cm^{-3}, and the experimental results are shown in Figure 3. When the defect state of the absorber layer varies in the range of less than 10^{14}cm^{-3}, the solar cell performance is better. When the defect state density exceeds 10^{15}cm^{-3}, more defect states are introduced, which leads to an increase in the carrier compound strength and makes the cell performance worse. However, in practice, it is difficult to reduce the defect density to a very small level, and the simulation results indicate that the absorber layer defect is set at 1×10^{14}cm^{-3}.

Authorized licensed use limited to: UNIVERSIDADE FEDERAL DO ESPIRITO SANTO. Downloaded on June 14,2022 at 09:47:05 UTC from IEEE Xplore. Restrictions apply.

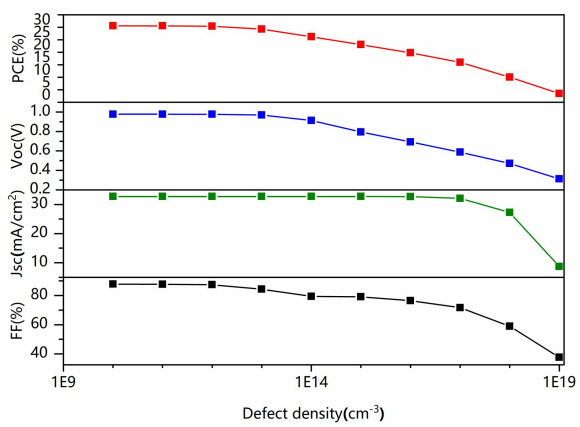

Figure 3. Effect of absorber layer defect density on cell performance

C. Effect of acceptor concentration (N_A) on cell performance

Sn-based perovskites are direct bandgap semiconductors with high absorption coefficients and narrow bandgaps, but as Sn^{2+} is easily oxidised to Sn^{4+}, P-type doping results in higher dark-state carrier densities, a process that can degrade device performance. The addition of SnO inhibits the formation of Sn^{2+} to Sn^{4+} [19-20]. Takashi et al. found that the acceptor density in the $CH_3NH_3SnI_3$ absorber layer can vary up to $10^{19}cm^{-3}$ [21]. Therefore, to investigate the effect of acceptor doping concentration on the performance of solar cells, J-V characteristic curves and plots of PCE with acceptor density 10^{14}~$10^{19}cm^{-3}$ are given in Figure 4.

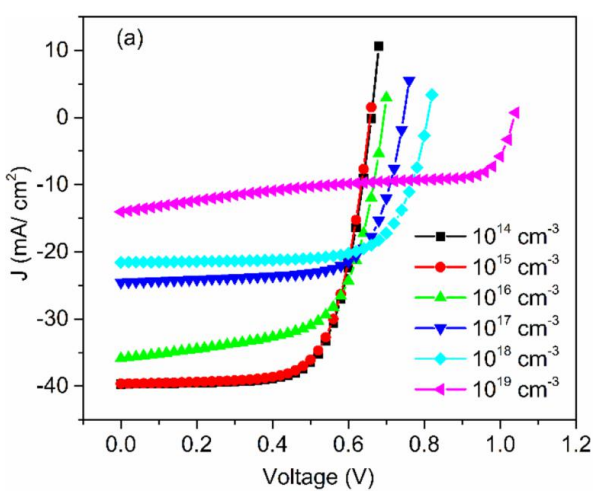

Figure 4. (a) J-V curve for different acceptor density

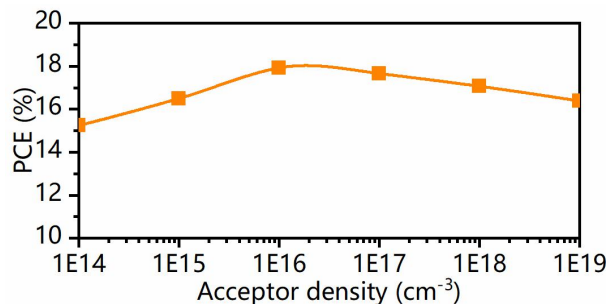

Figure 4. (b) PCE versus acceptor density.

When the acceptor density range is varied within 10^{16} cm^{-3}, the photovoltaic parameter changes very little, indicating that the photogenerated carrier production rate does not change with the acceptor density at the same photon number incidence. However, further as the acceptor doping concentration increases, the Fermi energy level of the hole decreases and therefore Voc increases, as shown in Fig. 4a. The decrease in Jsc with increasing acceptor doping concentration is probably due to an increase in the carrier complexation rate within the perovskite absorber layer. When the concentration exceeds $10^{16}cm^{-3}$, the PCE decreases rapidly and the defective state of the absorber layer leads to a significant decrease in power conversion efficiency, as shown in Fig. 4b. The results show that an appropriate defect density can improve cell performance; however, too high a concentration leads to a higher carrier recombination rate and poorer cell performance.

IV. Conclusions

SCAPS solar simulation software was used to simulate the performance of Sn-based perovskite solar cells. The simulation results show that too small a thickness of the absorber layer will limit the photovoltaic properties of the PSC due to insufficient absorption of photons, while too large a thickness of the absorber layer will affect the carrier transport and increase the carrier compound rate. On balance, the thickness of the absorber layer is 500 nm. Reducing the defect density of the absorber layer and improving Sn^{2+} stability are key issues for future research, which may be addressed by improving the fabrication techniques of the devices. The results show that an appropriate defect density can improve cell performance; however, too high a concentration leads to a higher carrier recombination rate and poorer cell performance. Better photovoltaic characteristics were obtained when the defect density of states was below $10^{14}cm^{-3}$. The optimised cell output characteristics are Voc = 0.917 V, Jsc = 33.14 $mA{\cdot}cm^{-2}$, and PCE = 23.93%, FF = 80.0%. The simulation results provide some reference ideas for the study of high-efficiency lead-free perovskite solar cells.

References

[1] Sun S Y, Salim T, Mathews N, Duchamp M, Boothroyd C, Xing G C, Sum T C, and Lam Y M. The origin of high efficiency in low-

Authorized licensed use limited to: UNIVERSIDADE FEDERAL DO ESPIRITO SANTO. Downloaded on June 14,2022 at 09:47:05 UTC from IEEE Xplore. Restrictions apply.

temperature solution-processable bilayer organometal halide hybrid solar cells. Energy Environ. Sci.,2014, 7: 399.

[2] D'Innocenzo V, Grancini G, Alcocer M J, Kandada A R, StranksS D, Lee M M, Lanzani G, Snaith H J, and Petrozza A. Excitons versus free charges in organo-leadtri-halide perovskites. Nat. Commun., 2014, 5: 3586.

[3] Maynard B, Long Q, Schiff E A, Yang M J, Zhu K, Kottokkaran R, Abbas H, and Dalal V L. Electron and hole drift mobility measurements on methylammonium lead iodide perovskite solar cells. Appl. Phys. Lett, 2016, 108: 173505.

[4] Yang D, Yang R X, Zhang J, Yang Z, Liu S Z, and Li C. High efficiency flexible perovskite solar cells using superior low temperature TiO2. Energy Environ. Sci. ,2015, 8: 3208.

[5] NREL. Best research-cell efficiencies. https: //www.nrel. gov/pv/ellfficiency.html, 2021.

[6] Philippe B, Park B W, Lindblad R, et al. Chemical and electronic structure characterization of lead halide perovskites and stability behavior under different expo-sures-A photoelectron spectroscopy investigation[J]. Chemistry of Materials,2015, 27 (5) ：1720-1731.

[7] Matsumoto F, Vorpahl S M, Banks J Q, et al. Photo-decomposition and morphology evolution of organomet-al halide perovskite solar cells[J]. Journal of Physical Chemistry C,2015,119(36) :20810-20816.

[8] Burgelman M, Decock K, Khelifi S, et al. Advancedelectrical simulation of thin film solar cells[J]. Thin Sol-id Films,2013,535(5):296-301.

[9] Zhang Q, Dandeneau C S, Zhou X, and Cao G. ZnO nanostructures for dyesensitized solar cells. Adv. Mater., 2009, 21: 4087.

[10] Lakhdar N, Hima A. Electron transport material effect on performance of perovskite solar cells based onCH3NH3GeI3 [J]. Optical Materials,2020,99 (1) :1-5.

[11] Patel, P. K. (2021). Device simulation of highly efficient eco-friendly ch3nh3sni3 perovskite solar cell. Scientific Reports, 11(1).

[12] Salem, Marwa. S., Ahmed Shaker, Abdelhalim Zekry, Mohamed Abouelatta, Adwan Alanazi, Mohammad T. Alshammari, and Christian Gontand. 2021. "Analysis of Hybrid Hetero-Homo Junction Lead-Free Perovskite Solar Cells by SCAPS Simulator" Energies 14, no. 18: 5741. https://doi.org/10.3390/en14185741

[13] Salah, M.M.; Hassan, K.M.; Abouelatta, M.; Shaker, A. A comparative study of different ETMs in perovskite solar cell with inorganic copper iodide as HTM.Optik2019,178, 958–963.

[14] Lin, L., Jiang, L., Li, P., Fan, B. & Qiu, Y. A modelled perovskite solar cell structure with a Cu2O hole-transporting layer enabling over 20% efficiency by low-cost low-temperature processing. J. Phys. Chem Solids 14, 205-211 (2019).

[15] Lazemi, M., Asgharizadeh, S. & Bellucci, S. A computational approach to interface engineering of lead-free CH3NH3SnI3highly-efficient perovskite solar cells. Phys. Chem. Chem. Phys. 00, 1-10 (2018).

[16] Son, D. Y., Im, J. H., Kim, H. S. & Park, N. G. 11% efficient perovskite solar cell based on ZnO nanorods: An effective charge col-lection system. J. Phys. Chem. C 118, 16567-16573 (2014).

[17] Du, H. J., Wang, W. C. & Zhu, J. Z. Device simulation of lead-free CH3NH3SnI3 perovskite solar cells with high efficiency. Chin. Phys. B 25, 108802-188809 (2016).

[18] Zhao, Z.et al. Mixed-organic-cation tin iodide for lead-free perovskite solar cells with an efficiency of 8.12%. Adv. Sci. 4,1700204-1700210 (2017)

[19] Hao, F. et al. Solvent-mediated crystallization of CH3NH3SnI3 films for heterojunction depleted perovskite solar cells. J. Am. Chem. Soc. 137, 11445-11452 (2015).

[20] Takahashi, Y., Hasegawa, H., Takahashi, Y. & Inabe, T. Hall mobility in tin iodide perovskite CH3NH3SnI3: Evidence for a doped semiconductor. J. Solid State Chem. 205, 39-43 (2013)

Authorized licensed use limited to: UNIVERSIDADE FEDERAL DO ESPIRITO SANTO. Downloaded on June 14,2022 at 09:47:05 UTC from IEEE Xplore. Restrictions apply.